

Award Accounts

The Chemical Society of Japan Award for Creative Work for 2002

Development of Ultrathin Polymer Films and Their Characteristics in Two Dimensions

Shinzaburo Ito,* Michiaki Mabuchi, Nobuhiro Sato, and Hiroyuki Aoki

Department of Polymer Chemistry, Graduate School of Engineering, Kyoto University, Katsura, Kyoto 615-8510

Received September 9, 2004; E-mail: sito@photo.polym.kyoto-u.ac.jp

Nanostructures and properties of ultrathin polymer films prepared by repeated deposition of monolayers have been investigated with emphasis on single chain morphology in two dimensions. The particular characteristics of ultrathin films were successfully revealed by novel optical microscopy and fluorescence spectroscopy techniques. A single polymer chain, which is confined into a two-dimensional plane, takes a contracted conformation, being segregated from other chains in the monolayer. Unlike three dimensional bulk polymers, there is little entanglement of polymer chains even for large molecular weight samples. These characteristics at the molecular level result in the entropy relaxation of individual chains with a small activation energy of diffusion, when the segmental motions are allowed at elevated temperatures. These understandings of structures and properties in two dimensions are indispensable for fabrication and application of polymeric thin films because the fine structures in low dimensions play critical roles in the production of advanced functions.

Recently, nanometric scale bottom-up chemistry has attracted much attention and various approaches have been taken to fabricate tailor-made architectures of materials from the atomic and molecular levels. Although this is a recent trend of the research projects originally initiated by the US government, fabrication of molecular architectures accompanied with various functions has always been a fascinating target in the field of chemistry. Polymeric materials, both biological polymers and synthetic polymers, have occupied an essential and indispensable position in this field of research because their secondary and higher order structures can be utilized as a major component of building blocks for molecular assemblies.

There are numerous strategies aiming at nano-fabrication from different point of views based on the scientific and technological backgrounds of individual researchers. The way we chose was the use of ultrathin polymer films. As schematically shown by colored films in Fig. 1, the multi-layered structure composed of extremely thin polymer films is able to control the distance of separation, sequence of layers, and orientation of molecules with a precision of nanometer scale in the direction of film thickness.[1–5] Furthermore, each layer could be modified with functional units such as chromophoric dyes, and electrochemically active donors and acceptors.[6–15] These functionalized ultrathin films allowed us to design and control some fundamental elementary processes concerned with the movement of excitons and electrons between the adjacent layers. It should be noted that these processes take place within a critical distance of only 1 nm. Therefore, precise control of spatial locations is absolutely required; in other words, it is necessary to develop homogeneous, defect-free, ultrathin films with a thinness of less than 1 nm.

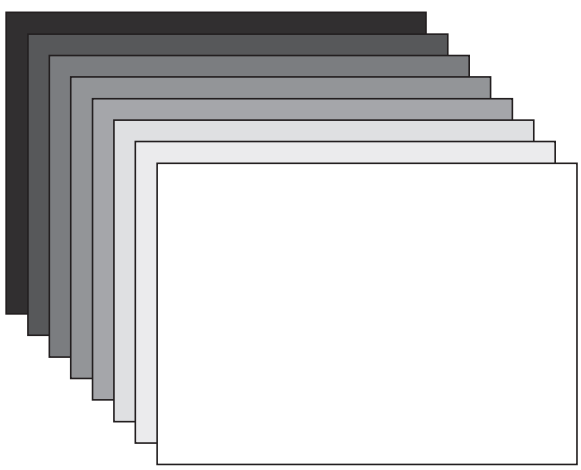

Fig. 1. Schematic illustration of ultrathin polymer films composed of monolayers deposited on a substrate.

In the 1980s, polymeric Langmuir–Blodgett (LB) films had been developed by several research groups.[16–20] The LB technique itself had already been established by the pioneering work of Langmuir and Blodgett, and then refined as an advanced molecular technology by Kuhn et al. in the 1960s.[21] Although it was a conventional and highly sophisticated technique, the emergence of novel polymeric materials based on polymer chemistry opened a new stage of LB films from a

Published on the web March 11, 2005; DOI 10.1246/bcsj.78.371

standpoint of functionality applicable to practical uses. Thinness, homogeneity, mechanical and thermal stability, variety of chemicals, ease of modification, so many advantageous characteristics of the polymeric films are provided by the intrinsic properties of amorphous polymers, which possess characters completely different from those of low molecular weight materials such as long alkyl fatty acids. Firstly in the next section, we will discuss the basic properties of polymer monolayer formed at the air/water interface.

During the course of studies on polymer monolayer and multi-layer films, however, we realized that abundant knowledge about three-dimensional polymer systems has been stored so far, but we have very little knowledge about two-dimensional polymers. The monolayer film, which has a molecularly ultimate thinness, can be regarded as a quasi two-dimensional plane, in which polymer chains must be restricted under the reduced freedom. It is obvious that the knowledge obtained from three-dimensional polymer science is not always applicable to understand the properties of ultrathin films. We can make a monolayer, but we do not know how the polymers behave in two dimensions. This simple question stimulated our motivation to the next research projects. In the current paper, we will discuss thermal and mechanical properties of ultrathin polymer films on the basis of morphology of single polymer chains imbedded into a planar space. Some experimental results elucidate the particular characteristics of two-dimensional polymer systems, which must be understood beforehand when we design and fabricate functional materials in a nanometer scale.

1. Polymer LB Films

The LB method is a unique and elaborate technique for fabricating molecular assemblies. Using amphiphilic molecules such as stearic acid, a monolayer is formed at the air/water interface under the balance of hydrophobic parts and hydrophilic units of the fatty acid, which are composed of long alkyl chains and carboxylic acids, respectively. The monolayer is transferred onto a solid substrate layer by layer. Even now, this wet process keeps the superior position as a method to build up organic molecular assemblies according to predetermined designs of architecture. In the 1980s, besides low-molecular-weight fatty acids, many amphiphilic polymers were also found to form stable monolayers on the water surface.[16–20] They were deposited on a solid substrate, e.g., a glass plate, silicon wafer, or plastic sheet, etc. by dipping the substrate into water as well as or more easily than the monolayers made from conventional low-molecular-weight amphiphilic molecules. Consequently, extremely thin polymer films were built-up in the desired order and also with an arbitrary number of layers, by the easy operation under moderate conditions. We call the layered films thus obtained on a substrate ultrathin polymer films, to distinguish them from the monolayers on the water surface.

Figure 2 shows the chemical structures of some amphiphilic polymers reported so far. In the main chain or at the side chain linked to the main chain, these polymers have hydrophilic substituents such as hydroxy, ester, amido, and ether groups, whose hydrophilic character is rather weak compared to the carboxylic acid used for low-molecular-weight LB films. Because the hydrophobic carbon–carbon main chain of polymers

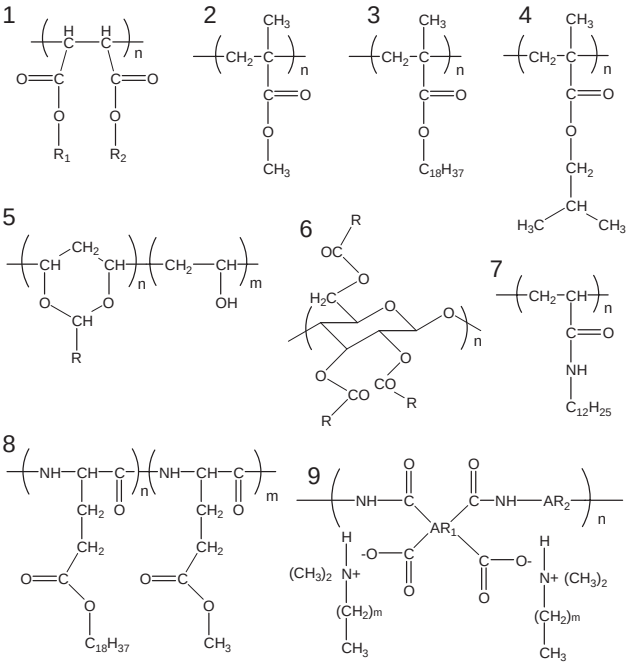

Fig. 2. Chemical structures of some representative polymers forming stable and transferable monolayers.

contributes to the cohesion of polymer segments, the long alkyl chain is not required as the hydrophobic part. Consequently, the film thickness of these polymer monolayers becomes very thin, mostly around 1 nm. Table 1 lists some important characteristics of polymer monolayers including film thickness. The polyimide monolayer achieved the thinnest value of only 0.4–0.5 nm, which is comparable to the thickness of the π-orbital of an aromatic ring.[19] The thickness observed in general corresponds to the molecular size evaluated for the monomer unit. Therefore, the term "polymer monolayer" refers to "a layer having a monomeric thickness in the respective polymer".

Another attractive point of ultrathin polymer films is found in the amorphous feature, in contrast to the crystalline character of fatty acid LB films. Owing to this particular characteristic, polymer monolayer and the ultrathin films possess various advantages: variety of chemical structure while keeping the amphiphilic character of film formation, homogeneous dispersion of functional groups introduced to the polymer chain,[8] thermal and mechanical stability after the deposition on substrates,[24] high electrical resistivity due to fewer defects of monolayer,[25] and so on. All these merits make the ultrathin films a promising candidate as a nano-component for fabricating molecular architectures.

The real image of a polymer monolayer can be observed with a Brewster angle microscope (BAM) in situ on the water surface.[26] Generally speaking, it is absolutely impossible to take a photograph of ultrathin films because there is no contrast between the area covered by a film and the bare surface. However, the use of p-polarized laser light, irradiating the surface at a critical angle of incidence, that is Brewster angle, allows one to distinguish the area as a result of a tiny difference of reflectivities.[27,28] Figure 3 shows two typical examples of polymer monolayers; the upper picture represents an image

Table 1. Characteristics of Some Polymer Monolayers Used for Preparation of Ultrathin Films

Polymer	Limiting area/nm^2 unit^{-1}	Thickness/nm	Surface pressure/mN m^{-1}[a)]	Ref.
3	0.27	3.0	20	16
4	0.28	1.1	12	18
5 (R = C_7H_{15})	0.31	1.05	30	17
6 (R = $C_{11}H_{23}$)	0.60	2.2	20	22
7	0.28	1.72	30	5
8	0.25	1.74	25	3, 23
9	1.7	0.5	25	19

a) Surface pressure at the deposition of monolayer.

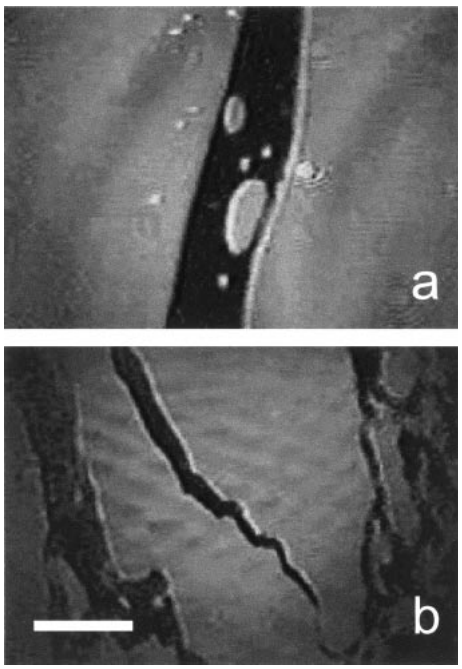

Fig. 3. Morphology of (a) PVD monolayer and (b) PODMA monolayer on water surface, observed by BAM at 0 mN m^{-1}. The bright area corresponds to the monolayer and the dark area to water surface. The scale bar is 100 μm.

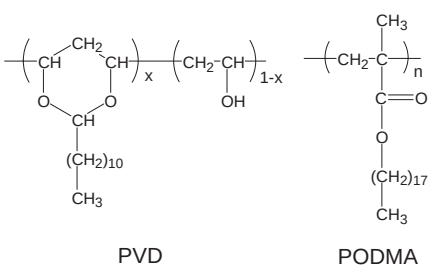

Scheme 1. Chemical structure of samples used for BAM imaging.

of a liquid-like monolayer of poly(vinyl dodecanal acetal) (PVD), and the lower picture is a crystalline-like monolayer of poly(octadecyl methacrylate) (PODMA). The chemical structures are shown in Scheme 1. In this figure, the black area corresponds to the bare surface of water with very low reflectivity under the Brewster angle irradiation, and the white part is the monolayer, providing a higher reflectivity of the incident light. The boundary of PVD monolayer looks very smooth and soft, which is easily deformed by the flow of water subphase, showing that this monolayer is in a liquid-condensed phase. On the other hand, the lower sample, PODMA, yielded a very rigid, solid-like monolayer. Although its plane looks very flat and perfect at the atomic level, there are many cracks with sharp edges like an ice plate, due to the strong cohesive forces among long alkyl side chains. It is known that the long side chains crystallize even though the main chains are in an amorphous state. In fact, the PODMA monolayer starts expanding and fusing on the water surface, when the water subphase is warmed up to 35 °C.[29] The liquid-like monolayers, as shown in the PVD image, are nicely transferred onto solid substrates without any cracks, and then stick like glue after drying. Thus the monolayer yields a stable and homogeneous ultrathin film. These optical images are very helpful for understanding the actual features of polymer monolayers.

2. Entanglement of Two Dimensional Chains

It is known that a polymer chain takes a random-coil conformation in three dimensions. However, when it is adsorbed on a surface by the attractive force between water and the hydrophilic units, each chain must change its conformation into a two-dimensional planar form in order to obtain the maximum enthalpy gain even though it loses conformational entropy. The thinness of monolayer indicates that this conformational change actually takes place at the interface. However, it is hard to imagine such conformational changes into two dimensions for a long chain molecule like a string. What kind of morphology does it take? And how is it packed on the surface and how does it make a monolayer film? BAM and surface viscosity measurements gave a clear answer to these questions. Figure 4 shows again a BAM image of a PVD monolayer, taken at a position close to the exit of the canal viscometer.[30] As shown in Fig. 5, a canal made of Teflon was placed on the water surface, and the monolayer was compressed from one side.[31] The monolayer shows noodle-like features at the exit, depending on its surface viscosity. The line-shape was deformed and spread again quickly for low-viscosity samples, but the shape for high-viscosity samples was kept for a long time and for a long distance from the spot of first appearance. Thus, the real image suggests that the surface viscosity measurement provides a good indication of morphology of polymer chains through the mechanical response of the monolayer.

Using the canal surface viscometer shown in Fig. 5, the surface viscosities of various monolayers were measured by ap-

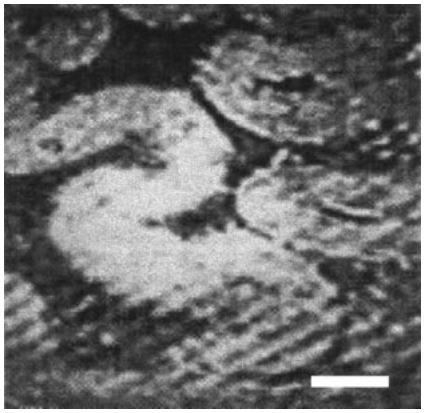

Fig. 4. Stripe-like domains observed at the exit of canal viscometer for a monolayer of poly(vinyl tetradecanal acetal). The scale bar is 100 μm.[30]

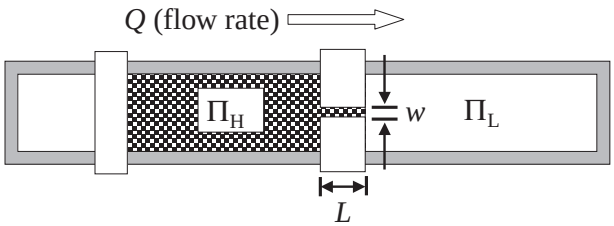

Fig. 5. A canal-type surface viscometer.

plying a small pressure difference, $\Delta\Pi = \Pi_H - \Pi_L$, between the left side and the right side of each surface. By monitoring the flow rate Q, defined by the surface area of monolayer passing through the canal in a unit time, as functions of canal width w, pressure difference $\Delta\Pi$, and subphase temperature, the surface viscosity η_s was evaluated with the following equation:

$$\eta_s = \frac{\Delta\Pi w^3}{12LQ} - \frac{w\eta_0}{\pi} \quad (1)$$

where η_0 is the bulk viscosity of subphase. Also the measurements were performed for a series of poly(vinyl acetal alkanal)s having various side chain lengths and molecular weights (Mw).[30] Figure 6 shows plots of surface viscosity vs side chain length of poly(vinyl acetal alkanal)s in the range of C4 (butanal) to C14 (tetradecanal). The number of methylenes has a marked effect on viscosity; the solid line represents the slope of dependence for reference. The increase in every four methylene units C_4H_8 results in one order of increase in the surface viscosity, showing the very strong cohesive force among hydrophobic alkane chains.

Figure 7 represents the Mw dependence of surface viscosity for poly(vinyl octanal acetal), which shows the linear dependence of viscosity over a wide range of Mw from 20 k to 1000 k.[32] Surprisingly, there is no inflection point at all; the slope was found to be around unity if the smallest Mw point is neglected. In three-dimensional systems, it is well known that the viscosity of polymer melts or concentrated solutions increases proportionally with the increase in Mw in the low Mw range, but shows a steep rise with the 3.4 power law for the Mw's larger than a critical mass Mc, at which polymer chains start entangling. Keeping this knowledge in mind let

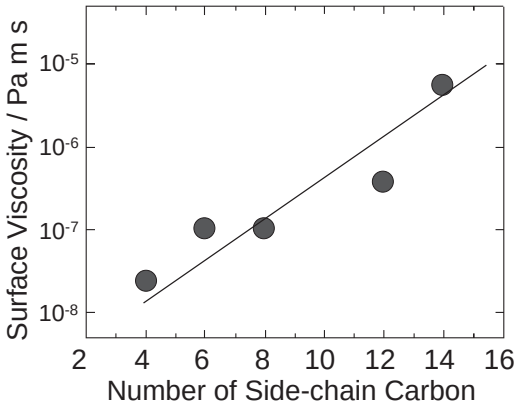

Fig. 6. Surface viscosity of PVAAs as a function of the side-chain carbon number. The solid line represents the steep rise in viscosity by a factor of 10 for each tetramethylene unit.[30]

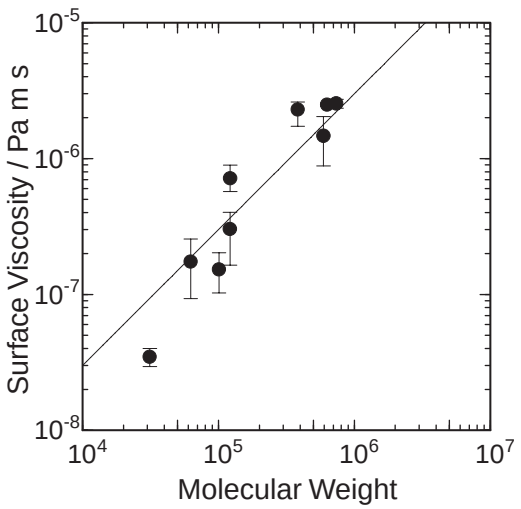

Fig. 7. Log–log plot of the surface viscosity vs the number average molecular weight. The solid line represents a slope of 1.0.[32]

us consider the two-dimensional system. The linear dependence of surface viscosity indicates that the polymer chains have very little entanglement in the monolayer. If chain entanglement occurs in two dimensions, the two chains would intersect with each other on the surface, and one chain would leave the surface to ride on the other chain. The experimental results indicate very low probability of appearance of such cross-entanglement, even for polymers with a large Mw of 10^6. Thus, the viscometric studies revealed that the strong attractive force at the air/water interface effectively unwinds the three-dimensional random coil of an individual chain, and lays it on the surface section by section with a two-dimensional planar form.

3. Single Chain Morphology in Two Dimensions

The next question is how does a polymer chain expand in two dimensions. To this question, de Gennes proposed a theoretical prediction that a two-dimensional chain segregates from others because the local concentration of single chain segments is independent of the degree of polymerization and is

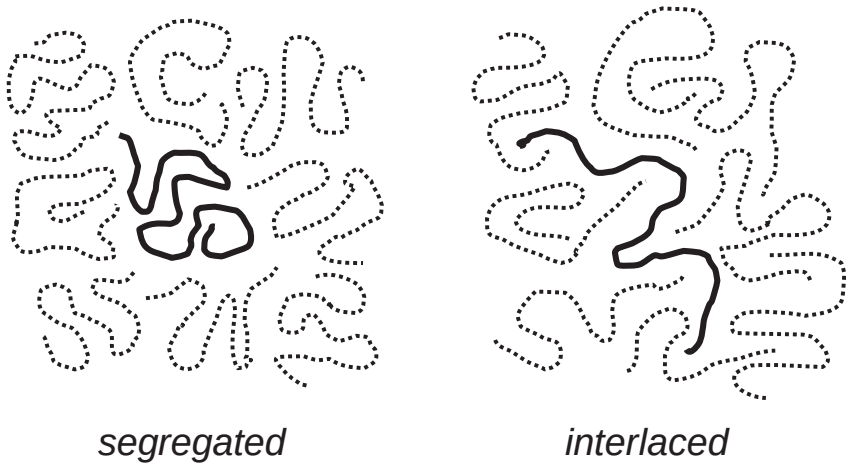

Fig. 8. Schematic illustration of chain conformations in two-dimensional monolayers.

equal to the total concentration of the polymer melt.[33] However, there had been no experimental evidence on chain conformations in two-dimensions, determining whether a single chain is segregated or interlaced. Figure 8 depicts a schematic illustration: in the left, a single chain is contracted and segregated from other chains; on the other hand in the right, the chains are interlaced with each other and expanded.

In order to investigate this issue, we employed the energy transfer method. The excitation energy transfer phenomenon has been used to evaluate the chain expansion parameters in solutions and in solids.[34–36] When a donor molecule is excited selectively, and there is no acceptor in close proximity, the donor emits fluorescence with a certain probability because the excitation energy is localized on it. But if an acceptor molecule is placed close to the donor, the energy efficiently transfers to the acceptor and then the acceptor emits fluorescence at a longer wavelength instead of the donor fluorescence. Therefore, the distance between two molecules R can be measured by fluorescence spectroscopy, because the transfer rate constant k_{et} is theoretically given by $(R_0/R)^6$, and the validity of the rate equation has been evidenced by many researchers. Therefore, the energy transfer method can be utilized as a spectroscopic nano-ruler and has been widely applied to various molecular assemblies, such as enzyme, membrane, and polymer systems.[37–40]

As to the study of polymer monolayers, a polymer chain was labeled with both the donor and acceptor chromophores at a fixed content, and the labeled polymer was diluted with a large amount of the same kind of non-labeled polymers so that energy transfer in an isolated single chain could be observed.[34] The more densely a polymer chain is contracted, the higher the energy transfer efficiency is expected, because of the shorter distance of separation between the donor and acceptor units. The polymer sample employed for this experiment was poly(isobutyl methacrylate) (PiBMA); the monolayer is in a liquid condensed state as mentioned above. A part of the side chains was labeled by both phenanthrene (P: donor) and anthracence (A: acceptor) chromophores with a few mole percents, as shown in Scheme 2. A dilute solution of PiBMA containing a trace amount of the labeled PiBMA was prepared. The mixed solution was spread on a water surface as usual, and the obtained monolayer was transferred onto

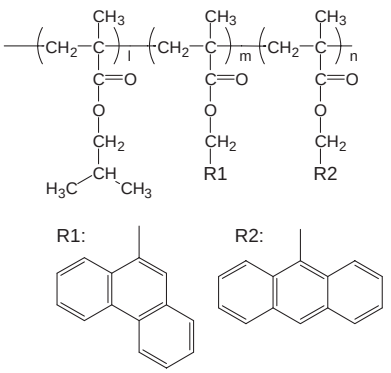

Scheme 2. Chemical structure of polymers labeled with fluorescent probes. The contents of probes are $m = 7\%$ and $n = 0.4\%$.

quartz substrates. To avoid the effect of interface, we covered the layer containing labeled chains with PiBMA monolayers on both sides, and we then examined the layer by fluorescence spectroscopy in order to determine the energy transfer efficiency between the donor and acceptor. Figure 9 shows the ratio, I_A/I_P, of the acceptor fluorescence intensity and the donor fluorescence intensity, which is a measure of energy transfer efficiencies, as a function of dilution with non-labeled PiBMA. The ratio gradually decreased with the degree of dilution, indicating that the inter-chain energy transfer was reduced by dilution. Above 50 times dilution, the ratio reached a constant value of 0.88, showing a value related to the intra-chain energy transfer efficiency for an isolated single chain. This intensity ratio was converted to the energy transfer efficiency, 0.19, by separate experiments using the same donor and acceptors.

The intra-polymer energy transfer efficiency thus obtained can be analyzed with respect to the root mean-square radius of gyration $\langle S^2 \rangle^{1/2}$ of two-dimensional polymer chains with the aid of a computer simulation based on the Monte Carlo method.[34] We used a model based on the self-avoiding walk on a two-dimensional hexagonal lattice, whose area is equal to the surface area of monomer unit, 0.21 nm^2, and whose number corresponds to the degree of polymerization, 512; both of these parameters could be determined by experiments. More

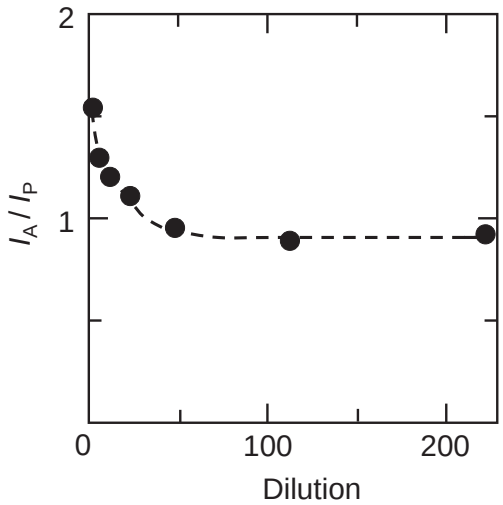

Fig. 9. Intensity ratios of the acceptor and donor fluorescence observed for samples with different dilutions. Energy transfer efficiency levels off at high dilutions, the value indicating intra-chain transfer efficiency.[34]

than 5000 chains for each expansion were generated on a computer, and the donors and acceptors were randomly distributed on the chain with a predetermined fraction of labels. All distances between the donors and acceptors were calculated, and finally energy transfer efficiency was evaluated for the chain expansion. These procedures are repeated, and then we took the statistical average of energy transfer efficiency related to the chain expansion parameters.

From this procedure, it was found that the transfer efficiency 0.19 corresponds to $\langle S^2 \rangle^{1/2} = 6.2$ nm. To discuss the chain morphology in relation to $\langle S^2 \rangle^{1/2}$, Fig. 10 shows some typical examples of two-dimensional conformation together with the $\langle S^2 \rangle^{1/2}$ values. Figure 10a presents a chain contracted due to strong cohesive forces among segments. On the other hand, Fig. 10c depicts an extended form generated under the self-avoiding random walk condition. Obviously, the extended chain has many voids, which are supposed to be filled with segments of other chains, if overlapping is allowed in two-dimensions. Figure 10b shows a snapshot of a chain conformation satisfying the experimental value of energy transfer, indicating that the chain in the monolayer takes rather contracted and segregated forms.

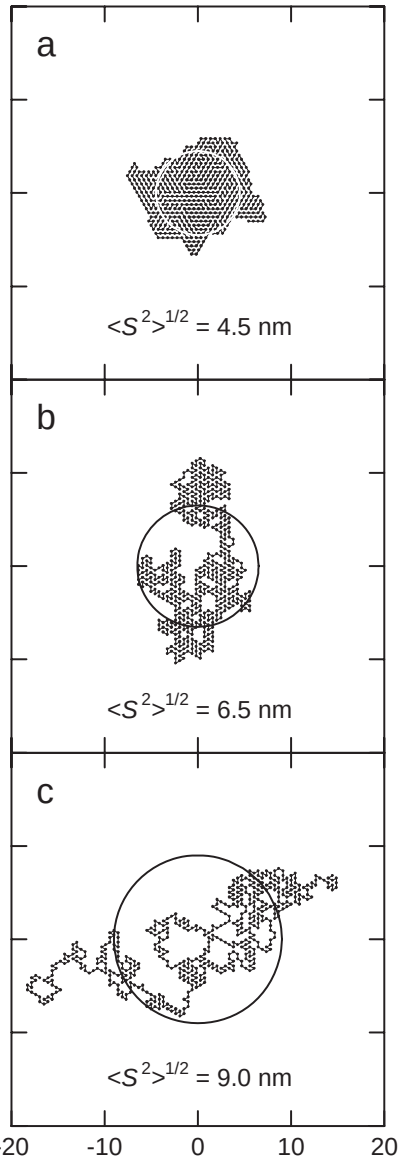

Fig. 10. A chain conformation simulated by computer. The radii of the circles correspond to the radius of gyration for each chain. The simulation was carried out with parameters for (a: top) the most contracted form and (c: bottom) the self-avoiding random walk model.[34]

4. Direct Observation of Single Chain Conformation

Recently, a novel optical microscope has been developed; it is called the scanning near field optical microscope (SNOM).[41,42] Details of the apparatus have been described elsewhere.[43–45] SNOM enables optical measurements with a high spatial resolution beyond the diffraction limit of light due to the confinement of near field emanating from a sharpened end of optical fiber. Light is not focused by a lens, but by a nanometric aperture of less than 100 nm in diameter. Owing to the advantage of an optical microscope, not only the surface but also the interior morphologies of objectives can be revealed with a high resolution under the ambient temperature and atmosphere. Therefore, the use of SNOM allowed us to take real images of a single polymer chain embedded in a monolayer.[46,47] PiBMA was again employed as the sample polymer examined, and was labeled by copolymerization of isobutyl methacrylate and 3-perylenylmethyl methacrylate; the feed of the latter fluorescent monomer was very small around 1%. The labeled polymer thus obtained, had a molecular weight of 3.3×10^6 with a polydispersity index of 1.23. It was diluted by a large amount of un-labeled PiBMA in order to isolate labeled chains in the two-dimensional matrix. The monolayer containing the labeled polymers was deposited on a quartz plate, and then subjected to SNOM measurements. Figure 11 shows a SNOM image of the monolayer with a dilution of 1/700. Several small but bright spots were observed with sufficient signal-to-noise ratios. The number of spots was increased proportionally with the increase in the concentration of labeled polymer, and the plane densities of bright spots were in

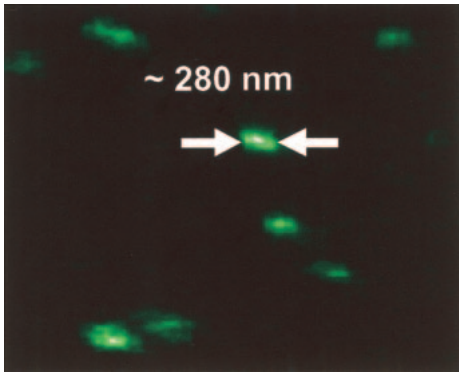

Fig. 11. SNOM image of single polymer chains embedded in a PiBMA monolayer.

agreement with those calculated from the surface area and the number of chains spread on the water. These results indicate that each spot represents a single polymer chain embedded in the PiBMA monolayer. The size of the spot is important. Obviously there are variations in both the size and the brightness, probably due to the polydispersity of molecular weight. However, the sizes of most spots observed were around 200–300 nm in diameter as seen in Fig. 11. Considering the very large Mw and the long contour chain length of 8000 nm, the small diameter provides unambiguous evidence that the polymer chain in a two-dimensional monolayer tends to take a contracted form, segregated from the surrounding chains. It is worth noting that if each chain takes a perfectly contracted conformation like a circle without other molecules inside, its diameter is estimated to be around 110 nm from the surface pressure–area isotherm and the degree of polymerization. These results are in good agreement with the conclusion derived by means of the energy transfer method in the previous section.

5. Structural Relaxation of Ultra-thin Films

Monolayer deposition on solid substrates is one of fascinating methods to fabricate artificial molecular assemblies of organic materials. Multi-layered ultrathin films obtained by successive deposition of extremely thin monolayers provide well-defined nanostructures, in which photochemical and electrochemical processes can be controlled by the design of geometrical arrangements of functional units incorporated with the monolayers. Compared with low molecular weight materials, the polymer films have much better thermal and mechanical stabilities of the layered structure, which is the most important subject for practical applications. However, it is absolutely true that the nanostructures based on the monolayer deposition are in a non-equilibrium state. Therefore they suffer inevitably from relaxation phenomena with aging time and thermal treatment after preparation. As described in the previous section, the energy transfer phenomenon is very sensitive to alteration of distances on a scale of nanometers. The same technique must be applicable to quantitative detection of the layered structure and its relaxation under elevated temperatures.[48–50]

A pair of layers containing the energy donor and acceptor chromophores was incorporated into spectroscopically inert layers, composed of the same kind of polymers but un-labeled with chromophores.[51] In this experiment, we used poly(vinyl

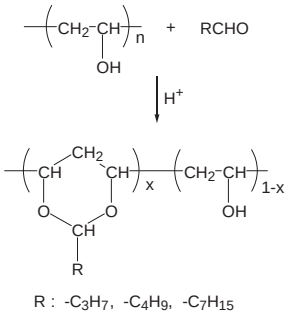

Scheme 3. Preparation of poly(vinyl alkanal acetal)s from poly(vinyl alcohol) with a degree of polymerization of 2000.

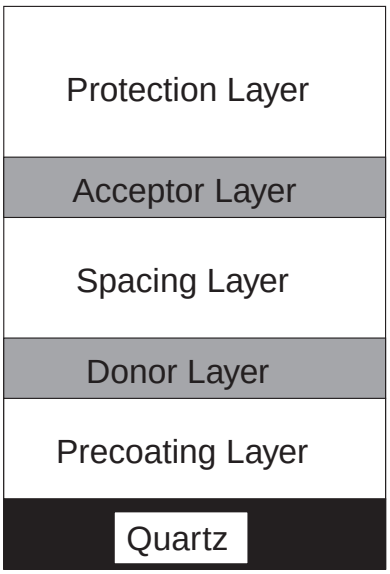

Fig. 12. Multi-layer structure for the energy transfer experiments.

alkanal acetal) (PVAA) that was synthesized by acetalization of commercial poly(vinyl alcohol). PVAA is useful as a base polymer because of the good transferability of the stable monolayer, and also owing to the ease of chemical modification at the side chains, to which various kinds of alkyl units and chromophoric groups can be introduced by a simple acetal reaction, as shown in Scheme 3. To examine the effect of glass transition temperature (T_g) of polymers on the relaxation behavior, we prepared three kinds of PVAAs with different lengths of the methylene units: poly(vinyl butanal acetal) (PVB), poly(vinyl pentanal acetal) (PVP), and poly(vinyl octanal acetal) (PVO). Figure 12 depicts the layer structure made for the interlayer energy transfer experiments. The sample was prepared in the following sequence: 4-layers of un-labeled polymer for precoating layers, 2-layers of phenanthrene (P) labeled polymers for the energy donating layers, n-layers ($n = 4$, 8) of un-labeled polymer for the spacing layers, 2-layers of anthracene (A) labeled polymer for the energy accepting layers, and finally $(10 - n)$ layers of un-labeled polymers for the protection layers. The films thus obtained have the same compositions of three component polymers, regardless of the spacing between P and A layers. The thickness of each layer was re-

ported as 0.85 nm for PVB, 0.90 nm for PVP, and 1.02 nm for PVO. Therefore, the distance of separation between the donor and acceptor layers can be arbitrary adjusted by the number of spacing layers n, with a precision of 1 nm.

Figure 13 shows fluorescence spectra for PVP film ($n = 8$) before and after annealing at 60 °C for 1 h. When the donor chromophore P was selectively excited at 298 nm, the fluorescence from P appeared at 350 nm and that of A was observed around 400 nm. The intensity ratio, I_A/I_P, on the spectra is a convenient measure of energy transfer efficiency. As shown in Fig. 13, the heat treatment gave rise to a drastic change of I_A/I_P, indicating thermal relaxation of the layered structure at the elevated temperature.

Figure 14 depicts the plots of normalized I_A/I_P on the course of heating of three samples with 8 spacing layers. Since the donor and acceptor layers were separated at the beginning, the intensity ratio I_A/I_P was very small, indicating the low energy transfer efficiency from an excited donor to acceptors. However, the transfer efficiency markedly increased at a critical temperature T_c, presented by the arrows in Fig. 14, showing that the donor-acceptor distances become closer than the initial state. The changes in the fluorescence spectra clearly evidenced that the layer structure was irreversibly disordered and mixed by the thermal treatment. The T_cs depended on the length of side chains. Table 2 lists the thermal properties of ultrathin films together with T_g of the bulk. The longer the side chain, the lower the value of T_g due to the flexibility of alkyl chains. Compared with the T_g of the corresponding polymer bulk, Fig. 14 indicates a close relationship between T_c and T_g. Consequently it is obvious that the polymer chains have very similar flexibility and mobility both in a bulk polymer and in an ultrathin monolayer.

The energy transfer method provides effective information not only about the distance of chromophores, but also about distribution of distances on the course of relaxation. Although the details of quantitative analysis have been described elsewhere,[48,49] the principles are noted here briefly below. Thermal treatment gives rise to interlayer diffusion of polymer segments, which results in a Gaussian distribution of chromophores along the direction normal to the layer plane as follows:

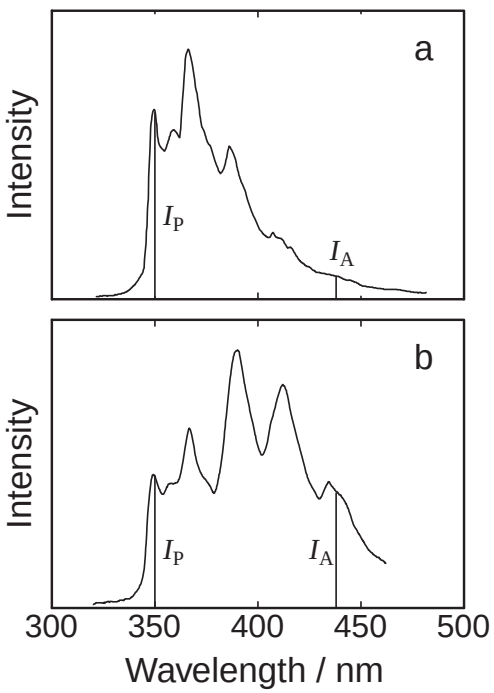

Fig. 13. Spectral changes of PVP films in which the donor and acceptor layers are separated with 8 spacing layers: (a) before annealing, (b) after annealing at 60 °C for 3 h.[49]

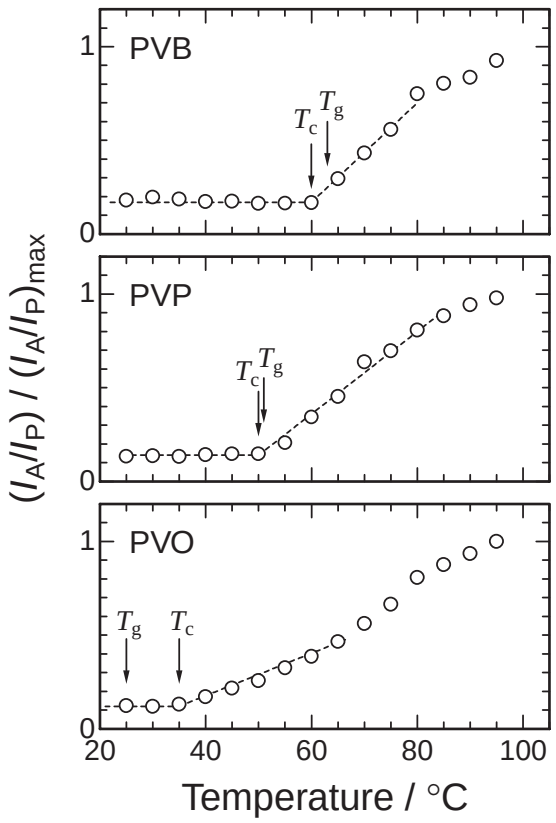

Fig. 14. Intensity ratios of the acceptor and donor fluorescence for PVB, PVP, and PVO samples during the first heating. The donor and acceptor layers were separated by 8 spacing layers at the beginning.[51]

Table 2. Thermal and Relaxation Properties of PVAA Ultrathin Films and the Bulk Polymer

Polymer	T_c /K	T_g /K	D[a] /10^{-16} cm^2 s^{-1}	$E_{a,LB}$ /kJ mol^{-1}	$E_{a,Bulk}$ /kJ mol^{-1}	Temperature range/K
PVO	308	298	2.5	70	180	313–333
PVP	323	324	0.5	120	240	333–353
PVB	333	336	<0.1	110	220	343–360

a) Diffusion constant obtained by the energy transfer method.

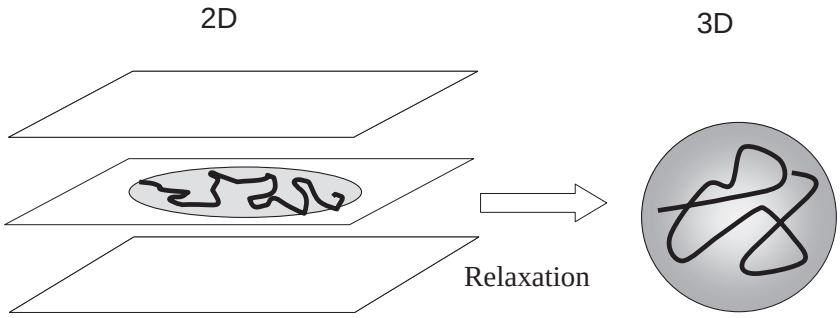

Fig. 15. Illustration of entropy relaxation from a two-dimensional planar conformation to a three-dimensional random coil conformation.

$$C(x) = \frac{C_0}{\sigma\sqrt{2\pi}} \exp\left(-\frac{(x - x_0)^2}{2\sigma^2}\right) \quad (2)$$

where $C(x)$ is the concentration of chromophores at a displacement x from the distribution center x_0, C_0 is related to the total number of chromophores in the system, and σ is the standard deviation of Gaussian distribution. Using this distribution function, the energy transfer efficiency under a given variance σ^2 for both the donor and acceptor layers was calculated numerically by a computer. The best fit of the theoretical transfer efficiency with the experimental data allowed us to determine the chromophore distribution in the multi-layered films. The variance σ^2 obtained as a result of fitting is related to the diffusion constant D for the Fickian diffusion model,

$$\sigma^2 = 2Dt + {\sigma_0}^2 \quad (3)$$

where σ_0 is the initial distribution of chromophores. Therefore, the measurement of time-dependent energy transfer efficiency at a constant temperature provides the time-dependent variance of distribution, and finally we can evaluate the diffusion constant D of the chromophores attached to the polymer chains.

The obtained values of D in Eq. 3 were in the order of 10^{-16}–10^{-17} $cm^2\,s^{-1}$, being very similar to the diffusion constant reported for a rubbery state of polymer bulk. The data were listed in Table 2. This result indicates again the similarity of the dynamics between the bulk and the ultrathin LB films. The Arrhenius plot of D for a PVO film showed a linear relationship of the logarithms of D against the reciprocal of temperature. From this slope, we obtained the apparent activation energy $E_{a,LB}$ for the diffusion process within a given temperature range, and $E_{a,LB}$ was compared with the activation energy for the bulk, $E_{a,Bulk}$ of the same polymer. The dynamic viscoelastic measurement is a useful method to analyze relaxation processes of polymer bulk. The storage modulus G' and the loss modulus G'' for three polymers: PVB, PVP, and PVO, were measured at an angular frequency ranging from 0.01 to 100 s^{-1} with a plate–plate type rheometer. According to the empirical principle of time–temperature superposition, the shift factor a_T was evaluated at various temperatures. The temperature dependence of a_T yields an Arrhenius form, with a linear dependence of $\ln a_T$ as follows:

$$E_{a,Bulk} = R\frac{d(\ln a_T)}{d(1/T)} \quad (4)$$

where $E_{a,Bulk}$ is the apparent activation energy for the relaxation process in the bulk. Table 2 also lists the $E_{a,Bulk}$ together with $E_{a,LB}$. The large difference between $E_{a,LB}$ and $E_{a,Bulk}$ is important; the former values are ca. half of the latter ones even for the same polymer. This significant alteration suggests that the different mode of molecular motions contributes to the relaxation processes. This phenomenon is explained as follows. When a monolayer was formed on the water surface, each individual polymer chain took a two-dimensional conformation, and then transferred onto a solid substrate. However, once the films were deposited and dried on the substrate, the polymer chains are free from the restriction to keep a two-dimensional conformation, which is now in a non-equilibrium state. Therefore, rearrangement proceeds in the films with a smaller activation energy compared with the relaxation of chains in an equilibrium state in the bulk. We may call this process "entropy relaxation" from a two-dimensionally restricted form to a three dimensional random coil conformation. Figure 15 illustrates the entropy relaxation of a chain confined to a plane at the initial state.

Another particular behavior of two-dimensional films was seen in the Mw effect on the relaxation process.[52] Similarly to the previous section, the energy transfer experiments were performed for PVO multi-layered films having a wide range of Mw from 1×10^4 to 2×10^5 with small polydispersities of 1.1, and the diffusion constant D was investigated as a function of Mw. Figure 16 shows the log–log plots at a couple of temperatures. As expected, the lower the temperature and also the larger the Mw, the smaller the diffusion constant D observed. However, the Mw effect on D was observed only in a low Mw region of less than 10^5; the value of D was independent of Mw in a higher Mw region. The slope of solid lines in Fig. 16 was ca. -2, indicating that the diffusion constant decreased with the inverse second power of Mw. This is quite natural behavior in various polymer bulk systems. Experimentally, for example, Whitlow et al. reported a similar tendency of self-diffusion coefficient of polystyrene at the interface of protonated and deuterated polymers.[53] Theoretically, the de Gennes's reptation model predicted the inverse second power dependence on Mw for entangled chains at long reptation times, at which the whole chain motions become predominant relaxation processes. Therefore, the result observed here indicates that the center of mass motion of the whole polymer chain contributes to the relaxation of nanostructures in the multi-layered film.

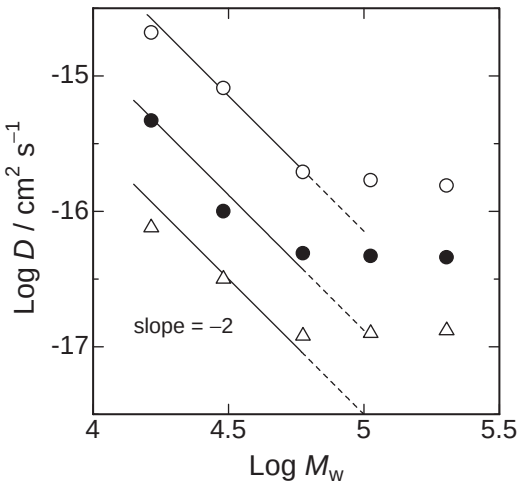

Fig. 16. Molecular weight dependence of diffusion constants at various temperatures: (○) 40 °C, (●) 30 °C, and (△) 25 °C.[52]

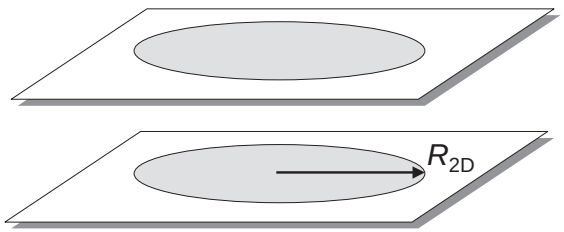

Fig. 17. Illustration of the layered structure and the size of a polymer chain contracted to a circular conformation.

On the other hand, the high Mw samples showed very little dependence on Mw. This strange behavior cannot be understood from the previous discussions based on the mass diffusion model of polymer chains. To explain this result, we need to take into account the size of chain and the thickness of film as shown in Fig. 17. As described in the previous section, a polymer chain in a two-dimensional plane tends to take a contracted form like a circle, and the minimum radius R_{2D} in plane was estimated from the surface area at the deposition pressure: $R_{2D} = 10.6$ nm for the largest Mw sample. Therefore, even in a shrunken form, the radius of a polymer chain exceeds the distance of separation between the donor and acceptor layers and becomes comparable to the total thickness of multi-layered films. This means that segmental motion of a part of chain is enough to disorder the whole layered structure. Consequently, the diffusion constant observed becomes independent of the molecular mass. It is worth noting that the smaller the size of the structure, the larger the contribution of segmental motions is. When the diffusion distance observed becomes shorter than the radius of gyration of a polymer chain, local motions come up as the rate-determining factor of the structural relaxation. As illustrated in Fig. 15, the local motions of two-dimensional chains are released at high temperatures close to T_g, and the polymer chain expands to a three-dimensional equilibrium form. This motion is quite effective to break the layered structure because the size of each polymer chain is large enough compared with the structures we made. These experiments revealed the mechanism of relaxation, which particularly appeared in two-dimensional polymer films. To prevent this disadvantage, one must suppress the segmental motion of polymer chains. Several approaches have been taken to obtain thermally stable films, for example, using rigid main chain polymers,[3,50] crosslinkable chains,[22,54] and self-organizing substituents at the side chains.[55] The wide range of variety in chemicals, synthesis, structures, physical properties, and interactions is always one of significant advantages of polymeric materials.

6. Concluding Remarks

The development of ultrathin polymer films has allowed one to fabricate well-defined nano-structures of organic materials. Besides the fine structure of the product, the wet and soft processes on preparation are suitable for a variety of materials, most of which are weak and broken under environments out of the ordinary atmosphere. Using this superior merit, ultrathin films can be modified with photofunctional and electrochemically active moieties, which are expected to undergo reactions in a desired manner by the nanostructures of the ultrathin films. Therefore, it is crucially important to know the exact inner structure and properties, although it is really difficult to investigate these matters because of the amorphous nature of polymeric substances. We employed optical and fluorescence methods which have a spatial resolution in the nanometer range, and also sensitive enough to detect weak signals from a monolayer. BAM, SNOM, and fluorescence probe methods provided invaluable unique information on the thin films. In this article, we first described the two-dimensional conformation of a single chain in a monolayer. The morphology and shear viscosity measurement on the water surface strongly suggested that polymer chains in a monolayer were segregated from other chains in two dimensions with little entanglement. These results were confirmed by intra-chain energy transfer measurements and optical microscopy, SNOM recently emerged. Both of these experiments indicated that a single chain embedded in a monolayer takes a contracted form like a pancake, in order to avoid formation of a free surface with vacancies under the dimensional restriction that individual chains cannot go across other chains lying on the water surface. This particular chain conformation in a two-dimensional plane was transferred onto solid substrates, yielding multi-layered ultrathin films. The layered structures, composed of pancake-like polymers, are obviously non-equilibrium structures on the substrate, which must inevitably be disordered by the segmental motions of polymer chains at elevated temperatures. The energy transfer method was used for monitoring the relaxation processes, and quantitative analysis based on the diffusion constants and their apparent activation energies revealed the mechanism of structural relaxation from a two-dimensional planar conformation to a random coil conformation. This process is caused by recovery of dimensional freedom associated with the increase of conformational entropy. Although relaxation phenomena are common to artificial assemblies, in general, the smaller size architecture must be subject to more rapid relaxation than the larger scale structures. This is also the case in polymer ultrathin films. Based on these results and appropriate selection of chemical structures, ultrathin films have

been developed as an indispensable component of functional nanomaterials.

References

1 R. H. Tredgold, *Thin Solid Films*, **152**, 223 (1987).
2 H. Ringsdorf, G. Schmidt, and J. Schneider, *Thin Solid Films*, **152**, 207 (1987).
3 G. Wegner, *Thin Solid Films*, **216**, 105 (1992).
4 "An Introduction to Ultrathin Organic Films," ed by A. Ulman, Academic Press, San Diego (1991).
5 T. Miyashita, *Prog. Polym. Sci.*, **18**, 263 (1993).
6 S. Ohmori, S. Ito, M. Yamamoto, Y. Yonezawa, and H. Hada, *J. Chem. Soc., Chem. Commun.*, **1989**, 1293.
7 S. Ito, H. Okubo, S. Ohmori, and M. Yamamoto, *Thin Solid Films*, **179**, 445 (1989).
8 S. Ohmori, S. Ito, and M. Yamamoto, *Macromolecules*, **23**, 4047 (1990).
9 S. Ito, S. Ohmori, and M. Yamamoto, *Macromolecules*, **25**, 185 (1992).
10 H. Ohkita, H. Ishii, S. Ito, and M. Yamamoto, *Chem. Lett.*, **2000**, 1092.
11 A. Aoki and T. Miyashita, *J. Electroanal. Chem.*, **473**, 125 (1999).
12 A. Aoki, Y. Tamagawa, and T. Miyashita, *Macromolecules*, **35**, 3686 (2002).
13 T. Ogi, H. Ohkita, S. Ito, and M. Yamamoto, *Thin Solid Films*, **415**, 228 (2002).
14 H. Okita, T. Ogi, R. Kinoshita, S. Ito, and M. Yamamoto, *Polymer*, **43**, 3571 (2002).
15 M. Ferreira, C. J. L. Constantino, C. A. Olivati, M. L. Vega, D. T. Balogh, R. F. Aroca, R. M. Faria, and O. N. Oliveira, *Langmuir*, **19**, 8835 (2003).
16 S. J. Mumby, J. D. Swalenand, and J. F. Rabolt, *Macromolecules*, **19**, 1054 (1986).
17 M. Watanabe, Y. Kosaka, K. Oguchi, K. Sanui, and N. Ogata, *Macromolecules*, **21**, 2997 (1988).
18 K. Naito, *J. Colloid Interface Sci.*, **131**, 218 (1989).
19 Y. Nishikata, A. Morikawa, M. Kakimoto, Y. Imai, K. Nishiyama, and M. Fujihira, *Polym. J.*, **22**, 593 (1990).
20 R. H. G. Brinkhuis and A. J. Schouten, *Macromolecules*, **24**, 1487 (1991).
21 H. Kuhn, D. Möbius, and H. Böcher, "Physical Methods of Chemistry," ed by A. Weissberger and B. W. Rossiter, Wiley (1972), Vol. 1, Part 3B.
22 T. Kawaguchi, H. Nakahara, and K. Fukuda, *Thin Solid Films*, **133**, 29 (1985).
23 M. Mabuchi, S. Kobata, S. Ito, M. Yamamoto, A. Schmidt, and W. Knoll, *Langmuir*, **14**, 7260 (1998).
24 S. Ito, T. Ueno, and M. Yamamoto, *Thin Solid Films*, **211**, 614 (1992).
25 Y. Budianto, A. Aoki, and T. Miyashita, *Macromolecules*, **36**, 8761 (2003).
26 S. Ito and M. Yamamoto, "New Macromolecular Architechture and Functions," ed by M. Kamachi and A. Nakamura, Springer, Berlin (1996), pp. 127–136.
27 S. Henon and J. Meunier, *Rev. Sci. Instrum.*, **62**, 936 (1991).
28 D. Hönig and D. Möbius, *J. Phys. Chem.*, **95**, 4590 (1991).
29 Y. Sakurai, N. Sato, S. Ito, and M. Yamamoto, *Kobunshi Ronbunshu*, **56**, 850 (1999).
30 N. Sato, S. Ito, and M. Yamamoto, *Polym. J.*, **28**, 784 (1996).
31 M. Sacchetti, H. Yu, and G. Zografi, *Rev. Sci. Instrum.*, **64**, 1941 (1993).
32 N. Sato, S. Ito, and M. Yamamoto, *Macromolecules*, **31**, 2673 (1998).
33 P. G. DeGennes, "Scaling Concepts in Polymer Physics," Cornell University, Ithaca, N.Y. (1979).
34 N. Sato, Y. Ohsawa, S. Ito, and M. Yamamoto, *Polym. J.*, **31**, 488 (1999).
35 G. Liu and J. E. Guillet, *Macromolecules*, **23**, 1388 (1990).
36 G. Liu, *Macromolecules*, **26**, 1144 (1993).
37 S. Ohmori, S. Ito, and M. Yamamoto, *Macromolecules*, **24**, 2377 (1991).
38 M. A. Winnik and F. M. Winnik, *Adv. Chem. Ser.*, **236**, 485 (1993).
39 Y. Rharbi and M. A. Winnik, *Macromolecules*, **34**, 5238 (2001).
40 J. P. S. Farinha, J. G. S. Spiro, and M. A. Winnik, *J. Phys. Chem. B*, **105**, 4879 (2001).
41 "Near-field Nano/Atom Optics and Technology," ed by M. Ohtsu, Springer, Tokyo (1998).
42 "Nano-Optics," ed by S. Kawata, M. Ohtsu, and M. Irie, Springer, Berlin (2002).
43 H. Aoki, S. Tanaka, S. Ito, and M. Yamamoto, *Macromolecules*, **33**, 9650 (2000).
44 H. Aoki and S. Ito, *J. Phys. Chem. B*, **105**, 4558 (2001).
45 H. Aoki, T. Hamamatsu, and S. Ito, *Appl. Phys. Lett.*, **84**, 356 (2004).
46 S. Ito, H. Aoki, and M. Anryu, *Trans. MRS-J*, **26**, 929 (2001).
47 S. Ito and H. Aoki, *Macromolecules*, submitted.
48 M. Yamamoto, K. Kawano, T. Okuyama, T. Hayashi, and S. Ito, *Proc. Jpn. Acad., Ser. B*, **70**, 121 (1994).
49 T. Hayashi, T. Okuyama, S. Ito, and M. Yamamoto, *Macromolecules*, **27**, 2270 (1994).
50 M. Mabuchi, S. Ito, M. Yamamoto, T. Miyamoto, A. Schmidt, and W. Knoll, *Macromolecules*, **31**, 8802 (1998).
51 M. Mabuchi, K. Kawano, S. Ito, M. Yamamoto, M. Takahashi, and T. Masuda, *Macromolecules*, **31**, 6083 (1998).
52 S. Ito, K. Kawano, M. Mabuchi, and M. Yamamoto, *Polym. J.*, **28**, 164 (1996).
53 S. J. Whitlow and R. P. Wool, *Macromolecules*, **24**, 5926 (1991).
54 K. Mathauer, A. Schmidt, W. Knoll, and G. Wagner, *Macromolecules*, **28**, 1214 (1995).
55 J. G. Meier, R. Ruhmann, and J. Stumpe, *Macromolecules*, **33**, 843 (2000).

Shinzaburo Ito, Professor at Kyoto University, was born in 1951. He graduated from Kyoto University in 1973 and obtained his doctoral degree of Engineering in 1981 from Kyoto University. He was appointed as a Research Instructor of Kyoto University in 1979. He experienced being a guest scientist of Max-Planck Institute for Polymer Research (Mainz) in the laboratory of Prof. W. Knoll from 1991 to 1992, and was also a visiting research fellow of RIKEN (Wako) during 1993–1999. He was promoted to Associate Professor in 1994 and to Professor of Department of Polymer Chemistry, Kyoto University, in 1999. His research interests encompass the polymer nano-structure, polymer photophysics and photochemistry, ultra-thin films and their optical and electrical properties.